Ordered $Co_{48}Pb_{52}$ Nanowire Arrays Electrodeposited in the Porous Anodic Alumina Oxide Template with Enhanced Coercivity

G. B. Ji, S. L. Tang,* B. X. Gu, and Y. W. Du

National Laboratory of Solid State Microstructure and Physics Department of Nanjing University, Nanjing 210093, China

Received: September 10, 2003; In Final Form: April 27, 2004

Co−Pb nanowire arrays with an average diameter of 20 nm and lengths up to several micrometers were grown in ordered anodic alumina templates using AC electrodeposition. The as-deposited samples were annealed at different temperatures. The structure and magnetic properties of Co−Pb nanowires were analyzed by X-ray diffraction and a vibrating sample magnetometer. We found that the sample annealed at 700 °C had large perpendicular coercivity *Hc* (as high as 2660 Oe) and high squareness (M_R/M_s) (about 0.97), which was much larger than that of pure Co nanowires annealed at 700 °C (2170 Oe, 0.9). The change in coercivity and squareness associated with the microstructure was discussed.

Introduction

The magnetic nanowires, fabricated by various methods, have recently attracted much attention due to their potential significant technological implications.[1−2] One promising technique with which to obtain nanomagnet arrays is based on the template method.[3] This approach entails synthesizing the desired metal or semiconductor nanowires within the hexagonally arranged porous anodic alumina oxide (AAO) templates. Among the methods reported, the electrodeposition technique is a viable processing route for the production of magnetic nanostructures in addition to the previously demonstrated techniques such as sputtering, chemical vapor deposition, and molecular beam epitaxy techniques. In particular, electrodeposition is suitable for fabricating arrays of magnetic nanowires into an AAO template where conventional deposition processes would present severe limitation in the filling efficiency such as time and cost-consuming vacuum.

We know there have been numerous publications about nanowire array filled porous AAO templates such as Fe,[4] Co,[5] and Ni[6] and ferromagnetic alloys such as FeCo,[7] FeNi,[8] and CoNi[9] electrodeposited in the AAO template. In addition, various multilayered nanowires including Co/Cu,[10] Ni/Cu,[11] NiFe/Cu,[12] CoNi/Cu,[13] and Ag/Co[14] have been studied intensively due to their interesting magnetic and transport properties. Heterogeneous ferromagnetic−nonmagnetic alloy films such as Co−Cu[15] and Co−Ag[16] grown by a variety of methods have also been investigated in detail. However, only a few studies on heterogeneous ferromagnetic−nonmagnetic alloy nanowire array systems exist in the literature. Among them, Bjythe et al.[17] have fabricated Co−Cu alloy nanowires and presented a preliminary study of their transport property. Fedosyuk et al.[18] reported on the granular deposited Ag/Co in porous anodic aluminum oxide that exhibited a magnetoresistance effect at room temperature. Recently, Wang et al.[19] have fabricated Fe−Ag and Co−Ag nanowire arrays embedded in the AAO template and showed the variation of the coercivities vs annealing temperature. Though there have been numerous publications about heterogeneous alloys, Co−Pb alloy systems have been scarcely reported in the literatures.

* To whom correspondence may be addressed. E-mail: gbji@ufp.nju.edu.cn.

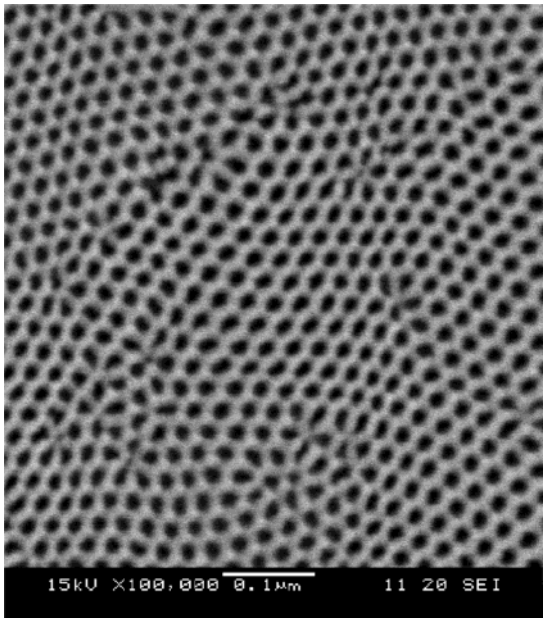

Figure 1. SEM images of anodic alumina oxide template with 20 nm diameter pores.

We report here the magnetic properties of $Co_{48}Pb_{52}$ nanowrie arrays prepared by electrodeposition in a porous AAO template. The enhance coercivity (2660 Oe) and perpendicular anisotropy appear in the sample annealed at the temperature of 700 °C which surpasses that of the pure cobalt nanowires. The XRD and differential thermal analysis (DTA) results also show that the microstructure varies at the annealing temperature of 700 °C.

Experimental Section

The ordered porous alumina membranes were prepared via an anodization process described in detail previously.[20] Aluminum forms a porous oxide with uniform and parallel pores when anodized in an acidic electrolyte. The hole interval of anodic porous alumina, in other words, the cell size, is determined by the applied voltage used for anodization. Figure 1 shows a typical scanning electron microscopy (SEM) micro-

10.1021/jp0367023 CCC: $27.50
Published on Web 05/28/2004

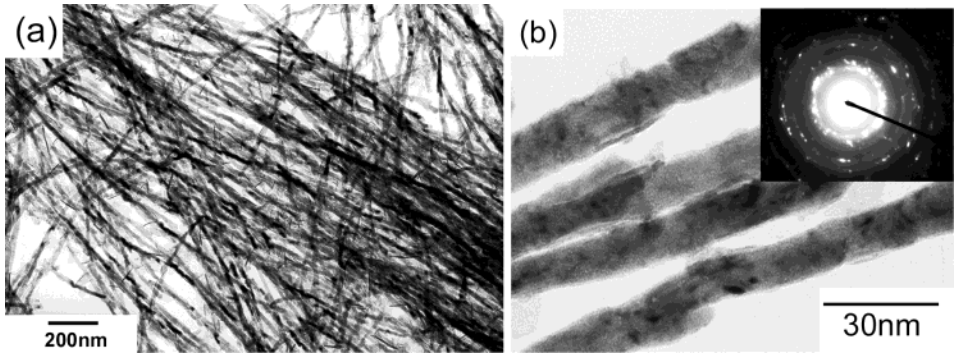

Figure 2. TEM images of the as-deposited Co−Pb alloy nanowires with a diameter of about 20 nm: (a) several Co−Pb alloy nanowires detached from the AAO template; (b) several parallel Co−Pb alloy nanowires, the inset is the SAED pattern taken from these nanowires.

graph of the AAO template, anodized using 0.3 M H_2SO_4 electrolyte at 0 °C and a voltage of 20 V. One can see that the anodic alumina template has almost arranged the pore array with the average diameter of the pores about 20 nm and the interpore distance about 35 nm.

The magnetic component is present at 48 atomic %. The composition was analyzed by induction-coupled plasma spectrometer. To achieve this composition in electrodeposited Co−Pb nanowires, the relative Co concentration has to be greatly increased owing to the extremely high rate of Pb deposition compared to that of Co. The electrolyte used to electrodeposit Co−Pb nanowires had the following composition: $Co(CH_3COO)_2 \cdot 4H_2O$, 30 g/L; $Pb(CH_3COO)_2 \cdot 3H_2O$, 6 g/L; H_3BO_3, 30 g/L with a pH value of 5.68. Deposition was carried out at room temperature with an AC voltage of 40 V, 50 Hz using a graphite counter electrode. Nanowires were electrodeposited in porous AAO membranes with the length range from 0.5 to 5 μm and the average diameter basically equal to that of the pores of the used template. After electrodeposition, the Co−Pb nanowire arrays were annealed for 20 min at different temperatures (300, 400, 500, 600, and 700 °C).

Results and Discussion

Transmission electron microscopy (TEM) was used to characterize the structure and morphology of the Co−Pb nanowires. Samples were prepared for TEM by dissolving the AAO matrix in 0.1 M NaOH. The resulting suspension was washed with distilled water and ethanol and resuspended in ethanol by sonication. Figure 2 presents a typical TEM image of the as-deposited Co−Pb nanowires. The nanowires are both very regular and uniform, with an average diameter of about 20 nm and the length up to several micrometers. Furthermore, the highly crystalline nature of the as-deposited samples was investigated by the selected-area electron diffraction (SAED) measurements and many individual nanowires were characterized. The diffraction spots/rings shown in the inset of Figure 2b confirms that the nanowires are polycrystalline, which are consistent with our XRD results.

The structural properties of the samples are studied by XRD using Cu Kα radiation. Figure 3 shows the XRD patterns of some selected samples of Co−Pb nanowire arrays with different heat-treatment temperature. The XRD measurement shows that all peaks ((111), (200), (220), and (311)) of our sample annealed below 700 °C are consistent with those of a typical structure of face-centered-cubic (fcc) Pb. The peak positions and their relative intensities are consistent with standard power diffraction pattern of fcc Pb, indicating that there is no preferred orientation and that the as-deposited samples are polycrystalline structure. Neither fcc nor hexagonal-close-packed (hcp) Co peaks are

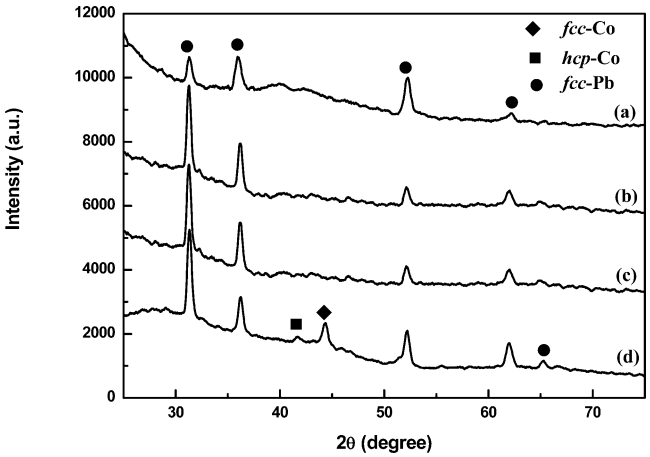

Figure 3. XRD patterns of electrodeposited Co−Pb alloy nanowires with different annealing temperatures: (a) 300; (b) 500; (c) 600; (d) 700 °C.

detected from the X-ray diffraction spectra in the annealing temperature range from 300 to 600 °C. Further annealing at 700 °C reveals a well developed fcc Co phase with the peak (111) and a small peak (100) that correspond to hcp Co (Figure 3d), indicating the existence of Co precipitates. We know that the Co−Pb represents an immiscible pair of materials under equilibrium conditions. However, under nonequilibrium conditions, the Co−Pb system could form metastable phase. From the XRD analysis, it is believed that the Co−Pb alloy nanowires are in a metastable phase below 700 °C due to the quick rate of electrodeposition under nonequilibrium conditions. The Co peaks appear in the sample annealed at 700 °C or above (see Figure 3d), suggesting a phase separation in this alloy system at or above 700 °C. This is similar to the Fe−Ag alloy, the Co−Ag alloy,[19] and the Co−Cu alloy.[21]

To investigate the phase transformation behavior in Co−Pb nanowires, subsequent DTA analysis has been carried out in Argon. Figure 4 shows a typical DTA curve of Co−Pb nanowires heated with 15 °C/min up to 800 °C. A distinct endothermic peak is seen at 650 °C. This temperature is believed to be the transformation temperature of the metastable phase. According to the XRD analysis, the metastable phase starts to separate into two phases at 650 °C or above.

The variation of perpendicular coercivity and squareness with annealing temperature (T_A) for the $Co_{48}Pb_{52}$ nanowires is shown in Figure 5a. The external field is applied parallel (//) to the long axes of the nanowires. As the annealing temperature increases from 300 to 600 °C, a very small change occurs in coercivity. However, we found that the perpendicular coercivity increases dramatically with the annealing temperature up to 700 °C and reaches a maximum (2660 Oe), which is larger than

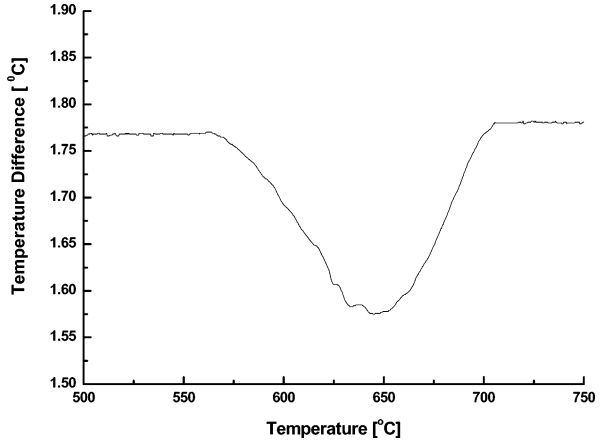

Figure 4. DTA curve of Co−Pb alloy nanowires in argon at 5 °C /min.

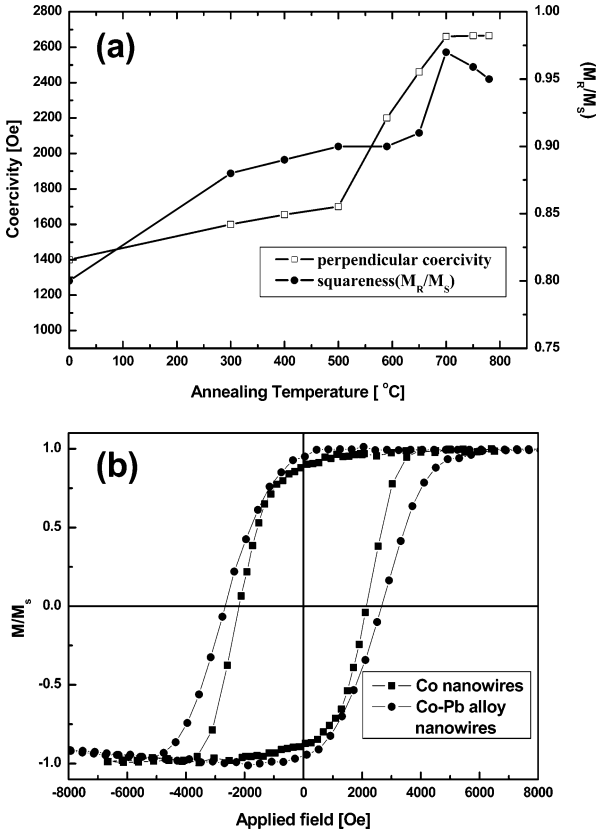

Figure 5. (a) he variation of perpendicular coercivity and squareness with annealing temperature for the Co−Pb alloy nanowires. (b) Typical hysteresis loop of ordered pure Co and Co−Pb alloy nanowire arrays annealed at 700 °C measured with an applied field parallel to the wires.

that of pure Co nanowires annealed at 700 °C. Figure 5b shows a typical $M-H$ loop of $Co_{48}Pb_{52}$ nanowires and pure Co nanowires in an anodic alumina template with an aspect ratio greater than 50 annealed at 700 °C measured in a magnetic field parallel to the nanowires. For the pure Co nanowires, the coercivity and squareness are found to be ∼2170 Oe and ∼0.9. It seems surprising that the $Co_{48}Pb_{52}$ nanowires show the enhancing magnetic properties. The effect of annealing temperature on the squareness is similar to that of coercivity.

The field dependent on magnetization was measured at room temperature by a superconducting quantum interference device magnetometer. Figure 6 shows the $M-H$ curves of the samples with the same volume annealed at different temperatures. The maximum applied field is 7 T. The saturation magnetization

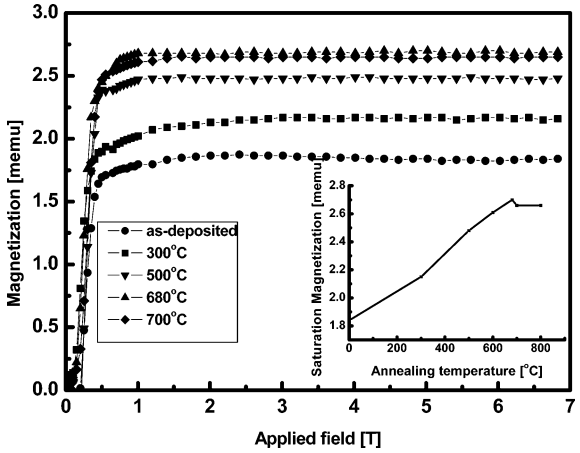

Figure 6. The field dependent on magnetization of the Co−Pb nanowires annealed at different temperatures for the field applied parallel to the nanowries. The inset is saturation magnetization (M_s) as a function of annealing temperature T_A.

(M_s) was obtained by extrapolating from high field $M-H$ curve. The saturation magnetization as a function of annealing temperature is shown in the inset of Figure 6. The saturation magnetization increases with increasing annealing temperature. The maximum value of M_s is 2.71 memu at T_A = 680 °C. However, the value of the saturation magnetization decreases slightly as the annealing temperature is further increased. The trend of change for M_s during the annealing process is similar to that for the coercivity. Those results prove for the view that the changes for M_s can be related to the precipitation of pure Co out of the Co−Pb nanowires.

The mechanism of this phenomenon is proposed as follows. The as-deposited samples have a number of defects due to the repaid AC electrodeposition. As the annealing temperature increases from 300 to 600 °C, the coercivity and squareness increase due to structural relaxation and reduction of defects. Above 700 °C, phase transformation occurs (see Figure 4): the Co−Pb alloy metastable phase is transferred to solid Co and liquid Pb. The Co grains recrystallize in liquid Pb. The sizes and shapes of Co grains are relatively uniform. Co grains have an average grain size of about 20 nm, which is close to that of the critical dimension for single domain, which consists of single Weiss domains. Higher coercivity might originate from nanocrystalline Co grains uniformly distributed in the nanowires. However, further annealing above 700 °C reaveals that the coercivity and squareness decrease slightly, which can be attributed to the oxidation.

Conclusions

In summary, we have studied the magnetic properties and microstructures of Co−Pb nanowire arrays fabricated by AC electrodeposition into AAO template. The $Co_{48}Pb_{52}$ nanowires annealed at phase transformation temperature exhibit a large perpendicular coercivity of 2660 Oe and a high squareness of 0.97, which are larger than that of Co nanowires.

Acknowledgment. This work was supported by Project No. 50171033 of National Natural Science Foundation of China and was a national key project of fundamental research (973, No. G 1999064508).

References and Notes

(1) Piraux, L.; George, J. M.; Despres, J. F.; Leroy, C.; Ferain, E.; Legras, R.; Ounadjela, K.; Fert, A. *Appl. Phys. Lett.* **1994**, *65*, 2484.

(2) Blondel, A.; Meir, J. P.; Doudin, B.; Ansermet, J. Ph. *Appl. Phys. Lett.* **1994**, *65*, 3020.

(3) Nielsch, K.; Muller, F.; Li, A. P.; Gosele, U. *Adv. Mater.* **2000**, *12*, 582.

(4) Yang, S. G.; Zhu, H.; Yu, D. L.; Jin, Z. Q.; Tang, S. L.; Du, Y. W. *J. Magn. Magn. Mater.* **2000**, *222*, 97.

(5) Zeng, H.; Zheng, M.; Skomski, R.; Sellmyer, D. J.; Liu, Y.; Menon, L.; Bandyopadhyay, S. *J. Appl. Phys.* **2000**, *87*, 4718.

(6) Nielsch, K.; Wehrspohn, R. B.; Barthel, J.; Kirschner, J.; Gosele, U.; Fischer, S. F.; Kronmuller, H. *Appl. Phys. Lett.* **2001**, *79*, 1360.

(7) Qin, D. H.; Cao, L.; Sun, Q. Y.; Huang, Y.; Li, H. L. *Chem. Phys. Lett.* **2002**, *358*, 484.

(8) Khan, H. R.; Petrikowski, K. *J. Magn. Magn. Mater.* **2000**, *215*, 526.

(9) Zhu, H.; Yang, S. G.; Ni, G.; Yu, D. L.; Du, Y. W. *Scripta Mater.* **2001**, *44*, 2291.

(10) Gravier, L.; Wegrowe, J. E.; Wade, T.; Fabian, A.; Ansermet, J. P. *IEEE Trans. Magn.* **2002**, *38*, 2700.

(11) Wang, L.; YuZhang, K.; Metrot, A.; Bonhomme, P.; Troyon, M. *Thin Solid Films* **1996**, *288*, 86.

(12) Dubois, S.; Marchal, C.; Beuken, J. M.; Piraux, L.; Duvail, J. L.; Fert, A.; George, J. M.; Maurice, J. L. *Appl. Phys. Lett.* **1997**, *70*, 396.

(13) Atterborough, K.; Hast, R.; Schwarzacher, W.; Ansermet, J. P.; Blondel, A.; Doudin, B.; Meier, J. P. *Mater. Res. Soc. Symp. Proc.* **1995**, *348*, 3.

(14) Valizadeh, S.; George, J. M.; Leisner, P.; Hultman, L. *Thin Solid Films* **2002**, *402*, 262.

(15) Kainuma, S.; Takayanagi, K.; Hisatake, K.; Watanabe, T. *J. Magn. Magn. Mater.* **2002**, *246*, 207.

(16) Zhang, W.; Boyd, I. W.; Elliott, M.; Herrenden-Harker, W. *J. Magn. Magn. Mater.* **1997**, *165*, 330.

(17) Blythe, H. J.; Fedosyuk, V. M.; Kasyutich, O. I.; Schwarzacher, W. *J. Magn. Magn. Mater.* **2000**, *208*, 251.

(18) Fedosyuk, V. M.; Kasyutich, O. I.; Schwarzacher, W. *J. Magn. Magn. Mater.* **1999**, *198*−*199*, 246.

(19) Wang, Y. W.; Zhang, L. D.; Meng, G. W.; Peng, X. S.; Jin, Y. X.; Zhang, J. *J. Phys. Chem. B* **2002**, *106*, 2502.

(20) Li, A. P.; Muller, F.; Birner, A.; Nielsch, K.; Gosele, U. *Adv. Mater.* **1999**, *11*, 483.

(21) Nguyen, A. T.; Nguyen, H. L.; Nguyen, C.; Vuong, V. H.; Nguyen, M. H. *Phys. B* **2003**, *327*, 400.